

Targeting observations with the quasi-inverse linear and adjoint NCEP global models: Performance during FASTEX

By ZHAO-XIA PU^{1*} and EUGENIA KALNAY²

¹*University Corporation for Atmospheric Research, USA*

²*National Centers for Environmental Prediction, USA*

(Received 7 October 1998; revised 29 March 1999)

SUMMARY

This note gives a brief summary of the targeting results obtained with both adjoint and quasi-inverse linear NCEP global spectral models during the Fronts and Atlantic Storm-Track Experiment (FASTEX). Questions concerning the feasibility of the methods and related issues about targeting observations are briefly discussed.

KEYWORDS: Adjoint Fronts and Atlantic Storm-Track Experiment (FASTEX) Quasi-inverse linear Targeted observations

1. INTRODUCTION

It has been shown that improvements in the initial analyses over data-sparse regions, such as oceans, can lead to significant improvements in forecasts over the continents downstream (e.g. Lord 1996). Because of limited resources, much attention has been given to determining the location where analysis errors would have the largest impact on the forecast for a particular region or synoptic phenomenon, and targeting this location for additional observations. The Fronts and Atlantic Storm-Track Experiment (FASTEX) (Joly *et al.* 1997) in January and February 1997 offered the first opportunity to test the feasibility of the general idea and the performance of different targeting techniques. The primary goal of this component of FASTEX was to improve the 24–48-hour forecasts of North Atlantic cyclones by providing additional dropsonde data in areas believed to be critical.

During the experiment, several techniques were tested in several operational centres to decide where the observations were most needed. These techniques were adjoint-based sensitivity and singular-vector calculations (e.g. Langland and Rohaly 1996; Palmer *et al.* 1998; Pu *et al.* 1998; Bergot *et al.* 1999), the quasi-inverse linear method (QILM) (Pu *et al.* 1997; Pu *et al.* 1998) and an ensemble transform (ET) technique (Szunyogh *et al.* 1999).

The National Centers for Environmental Research and Prediction (NCEP) participated in the FASTEX ‘upstream’ experiment by performing targeting experiments using, as a main strategy, the ET technique. In addition, the QILM and adjoint method (ADJM) with NCEP global models were used in real time. In a total of 15 upstream dropwindsonde missions with aircraft plans guided by NCEP during FASTEX, the ADJM was considered for the primary decision making nine times and the QILM was considered for five missions. The QILM and ADJM were also adopted partially in another six and five missions for flight plans, respectively (Toth 1997), while the ET technique was considered significant for the primary decision making 11 times.[†]

In this paper, we report on the results from both the ADJM and QILM during

* Corresponding author, present address: Universities Space Research Association, NASA Goddard Space Flight Center, Mail Code 912, Greenbelt, Maryland 20771, USA.

[†] During FASTEX, the NCEP team held a group meeting every day for decision making. The ET technique was chosen as the main strategy, and was considered essential for the flight plans. However, the ADJM and QILM sensitivity results were used as references so that these methods also influenced the decision making. The flight track usually fell into the area where the maximum sensitivities from all targeting techniques were collocated. As a result, even though in the decision making the ET method had the most significant role, most of the flight plans were overlapped by two or three targeting methods among ET, ADJM and QILM. On the other hand, there

FASTEX. Since the forecasting evaluation of NCEP targeting results has already been demonstrated in Szunyogh *et al.* (1999) with the ET technique, we do not present the detailed results of forecast impacts in this brief paper, but complement it by focusing on the method and areas of sensitivity for both ADJM and QILM during real-time FASTEX (section 2). The targeting results are presented in section 3, and a summary in section 4.

2. THE PERFORMANCE OF THE ADJOINT METHOD AND THE QUASI-LINEAR INVERSE METHOD DURING FASTEX

(a) Methodology

The ultimate goal of targeting observations is to improve the initial conditions by taking additional data where it can be most beneficial in improving the forecast skill in an area of large forecast uncertainty. Therefore, in general, three steps are needed for a successful targeted observation strategy: 1) A synoptic event of large forecast uncertainty has to be selected. This can be done by selecting, for example, a rapidly developing storm, and comparing different forecasts (from a single centre ensemble, or from forecasts originating in different operational centres) to assess the uncertainty of the forecast. 2) The optimal location and time of the targeted observations have to be identified using one or more techniques. 3) The extra observations have to be made available and assimilated in real time. Once the synoptic event has been chosen, the crucial question for the targeting experiment becomes: 'What is the optimal location for targeted observations?' i.e. 'where are the observations most needed?'. This problem can be posed as a forecast-error sensitivity problem (Rabier *et al.* 1996): find the location where changes in the initial conditions produce the largest forecast changes in the area of uncertainty. In other words, trace back the area of forecast uncertainty at the verification time, t_v , to a previous time (targeting time, t_t , or initial time, t_0). For example, suppose we can quantify the estimated forecast uncertainty, δX_v , at the verification area from the difference between two forecasts, or between a forecast and the verifying analysis. The corresponding sensitivity problem can be posed in two ways (Pu *et al.* 1998):

(a) *ADJM — gradient sensitivity or adjoint method.* Find the targeting area to which the forecast uncertainties at the verification time are most sensitive at the targeting time using the adjoint operator. In this method, the target locations are defined by the gradient of a forecast-error measure, J , with respect to its initial (or target) time t_t : The cost function is defined by $J = 1/2 \delta X_v^T W \delta X_v$. Where W is the weight that defines the error norm, J , over the verification area. The superscript 'T' denotes the transpose. In this paper, J is defined by a total-energy norm, multiplied by a local mask over the area of verification. $\delta X_v = L(t_t, t_v) \delta X_t$, where $L(t_0, t_1)$ is the tangent-linear model that advances a perturbation from time t_0 to t_1 . The gradient is given by an adjoint integration of the perturbation at the verification time, $\nabla_{x_t} J = W^{-1} L^T W \delta X_v$. Here, L^T is the transpose (adjoint) of L . The utility of this calculation in general is that the gradient shows the location where small changes to the initial conditions at targeting time have the greatest impact on the forecast error at verification time.

(b) *QILM sensitivity.* Define directly the change at the targeting time that leads to changes in the forecast verification area by the QILM, i.e. $\delta X_t = L^{-1} \delta X_v$. Here L^{-1} is a quasi-inverse linear operator, i.e. simply run the tangent-linear model backwards by changing the sign of Δt , while also changing the sign of the dissipative terms to avoid

were also a few missions that were guided by ADJM or QILM only or by ET only, provided the sensitivity results agreed with the corresponding sensitivity results from the European Centre for Medium-Range Weather Forecasts (ECMWF) or Meteo-France.

computational instability. For details see Pu *et al.* (1997) and Reynolds and Palmer (1998). It traces back the forecast difference, δX_v , over the verification area back to its corresponding initial (or targeting time) error, efficiently.

Since the forecast errors are unknown in real time for a specific synoptic event, in targeting applications the method takes the difference between two forecasts in the region of forecast uncertainty, setting the difference outside this area of interest to zero. The regional difference is then traced back to mark the location occupied by the corresponding initial changes. The targeted data will be taken in the area of large changes at the targeting time pointed out by either the ADJM or the QILM.

(b) *Configurations of experimental design during FASTEX*

At NCEP, large forecast uncertainties can be recognized using the NCEP global ensemble forecast system (Toth and Kalnay 1997). With the ADJM and/or QILM, the following procedures can be executed in order to determine the area where the observation will be taken, and they were followed during FASTEX:

(a) In general, the ensemble system alerts the forecasters about a crucial, but uncertain, storm development in the next few days (day 2 to 5 from initial time referred to as the verification time). A smooth mask centred in this area with an appropriate radius defines the area of interest. However, for FASTEX a mask with radius 1000 km centred at the pre-chosen location (50°N , 10°W) defined the area of interest.

(b) Select a pair of the ensemble forecasts which represent the largest ensemble differences and subtract one member of the ensemble from another, obtaining a forecast difference, and multiply by the masking filter (with a value close to one inside the mask and zero outside). In this way we obtain a localized ensemble forecast difference.

(c) The localized difference is used as an initial condition for a backward integration in two different ways: ADJM and QILM. The backward integrations trace back in time the verifying-time differences to their region of origin (at the targeting time, 1 or 2 days after the forecast initial time). This gives areas of large sensitivity patterns or perturbations that are considered as potentially optimal locations for targeted observation to be taken. These locations are used in the final decision making for aircraft dropsonde flight plans.

During FASTEX we performed the sensitivity calculations at 00 UTC and 12 UTC, with both the ADJM and QILM. Starting from the day 3 (T+72) ensemble forecast differences, we integrated both models back to T+60, T+48, T+36, T+24 and T+12. The operational forecast from the NCEP operational Medium-Range Forecast (MRF) model was used as a trajectory for the ADJM and QILM backward integrations. The adjoint sensitivity was the gradient at targeting time, based on a cost function defined by a total-energy norm. The QILM sensitivity was given by the perturbation at the targeting time calculated by the backward integration of the tangent-linear model. We used vertically averaged kinetic-energy values of the sensitivity fields over sigma levels 7–18 (from about 850 mb to 250 mb) to display the sensitivity map which was used for the decision making.

The model used for the sensitivity calculation was the NCEP operational global spectral model (i.e. MRF model) with a resolution of T62 and 28 sigma levels. The tangent-linear and ADJM models are the adiabatic versions with a minimum set of physics: horizontal diffusion, vertical mixing and surface drag, as in Pu *et al.* 1997.

TABLE 1. PRELIMINARY SUMMARY OF THE NCEP UPSTREAM FLIGHT PLAN

Intensive Observation Period	Flight take-off time	Forecast verification time	NCEP ensemble-transform method	NCEP adjoint method	NCEP quasi-inverse linear method	ECMWF singular-vector decomposition	France singular-vector decomposition	Forecast impact
2	1300 UTC 11 January	0000 UTC 13 January	Y	L	L	Y		
3	1000 UTC 13 January	1200 UTC 14 January		Y	L	Y		See Table 2
5	0900 UTC 20 January	1200 UTC 21 January		L	Y	L	Y	See Table 2
9	2200 UTC 31 January	1200 UTC 03 February	Y				Y	Szunyogh <i>et al.</i> 1999
11a	1000 UTC 04 February	0000 UTC 06 February 1200 UTC		L	L		Y	
11b	1200 UTC 04 February	0000 UTC 06 February 1200 UTC	Y	L			Y	Szunyogh <i>et al.</i> 1999
11c	0800 UTC 05 February	1200 UTC 07 February 0000 UTC			L	Y		See Table 2
11d	0000 UTC 06 February	1200 UTC 07 February 0000 UTC	Y		L			See Table 2
12	0900 UTC 09 February	1200 UTC 10 February	Y	Y		Y		
13	0800 UTC 10 February	1200 UTC 11 February	Y	L	Y	Y		Szunyogh <i>et al.</i> 1999 and Table 2
14	0800 UTC 12 February	0000 UTC 14 February		Y		Y	Y	See Table 2
15	1100 UTC 14 February	0000 UTC 16 February	Y	Y	Y			Szunyogh <i>et al.</i> 1999 and Table 2
16	0900 UTC 16 February	1200 UTC 17 February	Y	Y	Y	Y		Szunyogh <i>et al.</i> 1999 and Table 2
17	2200 UTC 17 February	0000 UTC 19 February	Y		P			Szunyogh <i>et al.</i> 1999
18	2200 UTC 21 February	1200 UTC 23 February	Y	Y	L	L	L	Szunyogh <i>et al.</i> 1999 and Table 2
19	2200 UTC 25 February	1200 UTC 27 February	Y,P	Y	Y		Y	See Table 2

Y: a substantial part of the flight was over strong-sensitivity areas indicated by the method, but this does not mean that all of the area of strong sensitivity was covered. P: only part of the flight was over strong-sensitivity areas. L: at least part of the flight was over a somewhat-sensitive region, often in these cases there was sensitivity in the area but there was a different area which appeared significantly more sensitive. A blank entry indicates that either the calculation was not available at the time of the decision making or the flight did not cover the sensitive region.

3. TARGETING RESULTS

(a) Sensitivity results

Table 1 gives a summary of the NCEP upstream experiments and the targeting guidance that were considered significant in the decision making. During FASTEX, the NCEP team also received some sensitivity maps from ECMWF and Meteo-France. Both

sensitivity results were calculated by an adjoint-based singular-vector decomposition method. Those results were also used as references for decision making, and are included in Table 1. The impacts of many of these cases were studied by Szunyogh *et al.* (1999) and are not repeated here. Figure 1 shows the sensitivity maps for those cases in which the ADJM or QILM was considered in real time in making the flight decisions, together with the flight paths. Table 2 gives further information about the FASTEX cases investigated in this study. It includes a summary of the assessment of the impact of the targeted observations. We should also mention that, of all the upstream NCEP experiments, IOP9 (Intensive Observation Period 9) was the case that showed the most improvement to the verification forecast. Unfortunately, neither ADJM nor QILM were run in time for flight decisions due to a computer-power shutdown, but a computation performed a posteriori showed that in this case their most sensitive regions agreed with the area indicated by the NCEP ET technique (not shown). Within the total 15 flight missions for NCEP strategy, we found that, in most cases, the ADJM and QILM supported the sensitivity results from the ET method. In the cases for which ET was not used, the NCEP ADJM and/or QILM identified areas for targeting that were in agreement with adjoint singular-vector sensitivity areas obtained by one or more of the other centres (ECMWF or Meteo-France).

(b) Forecast impact

The forecast impact was investigated using the current (February 1997) NCEP operational lower-resolution model, T62/L28, and three-dimensional variational analysis (i.e. SSI, Parrish and Derber 1992). Two, otherwise identical analyses and ensuing forecasts were made for each of the IOPs, with the extra targeted dropsonde data included (experimental) in one and excluded (control) from the other analysis. The evaluation of the targeted observations for most cases of NCEP missions has already been done for the NCEP ET technique (Szunyogh *et al.* 1999). In particular, the results for IOP13, IOP15, IOP16, and IOP18 are also valid for the ADJM and/or QILM, since they pointed out the same area of sensitivity as the ET method. In addition, we have done similar calculations for IOP3, IOP5, IOP11c and IOP11d, IOP14 and IOP19 (Table 2). The main results are summarized briefly as follows:

(a) For most of the cases, the initial signal introduced into the analysis by the targeted data, in the area found to be most sensitive, reaches the verification region at the verification time (figures not shown). Moreover, signals from adjacent areas usually have significantly less influence than those from the most sensitive region (see details in Szunyogh *et al.* (1999)).

(b) Following Szunyogh *et al.* (1999), we have checked the forecast verification against analysis field by checking the absolute forecast-error reduction in the surface pressure. The forecast impact, however, was mixed in most cases (Table 2). We also checked the root-mean-square fit of the forecasted wind field against all available radiosonde data between the surface and 250 hPa heights. Five out of ten cases (IOP5, IOP11c, IOP13, IOP18 and IOP19) show relatively clear positive impact. In particular, three out of five QILM cases show positive impact and three out of eight of ADJM case show positive impact.

4. SUMMARY AND DISCUSSION

The NCEP global spectral QILM and ADJM models were used in real time during FASTEX. Both methods were considered useful in determining the destination for the

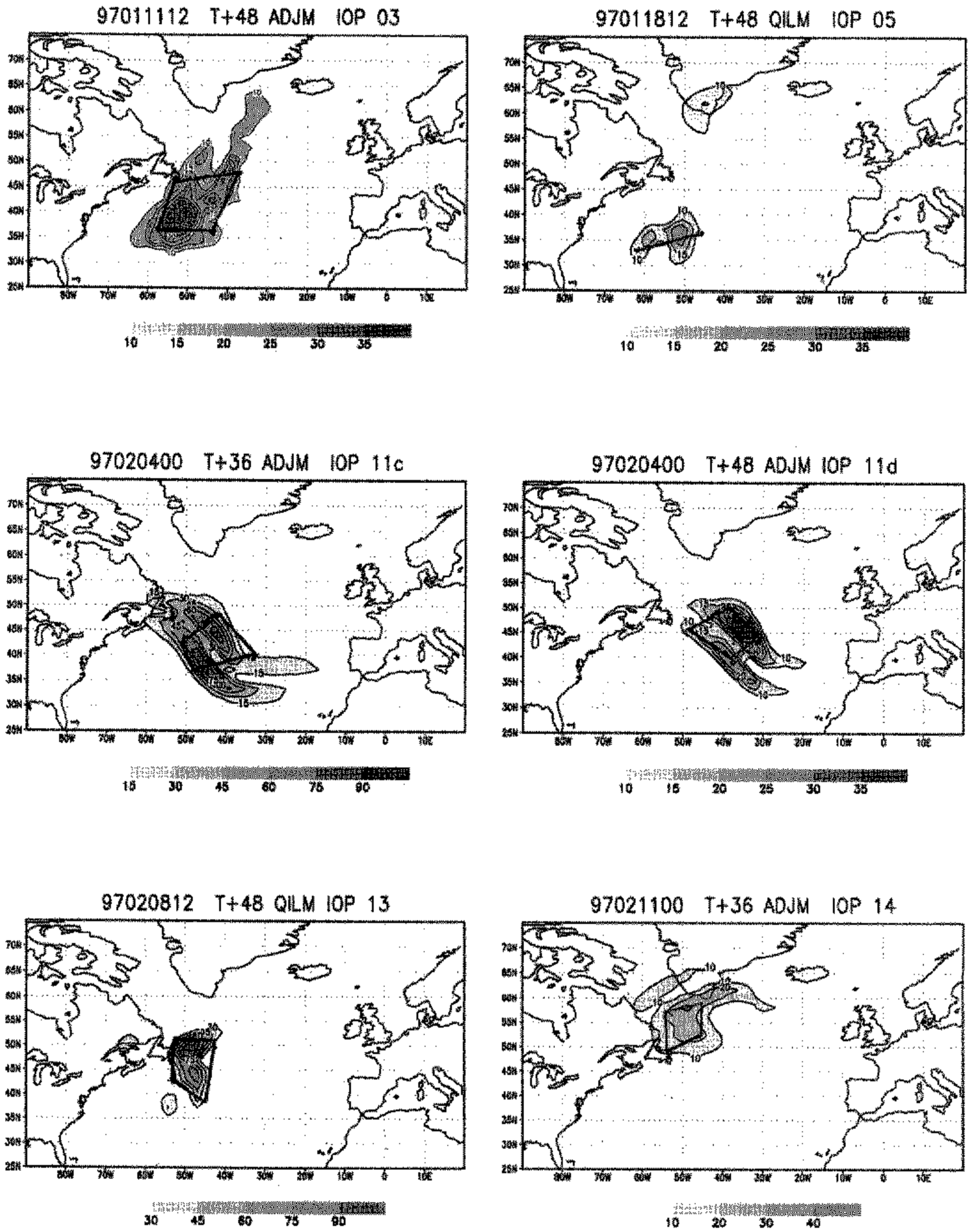


Figure 1. The sensitivity maps used for the flight decisions in real time, The contour interval is 5.0×10^{-2} (or 1.0×10^{-1}) $m^2 s^{-2}$ in ADJM sensitivity and $50 m^2 s^{-2}$ in QILM sensitivity. The flight track is marked by a bold solid line.

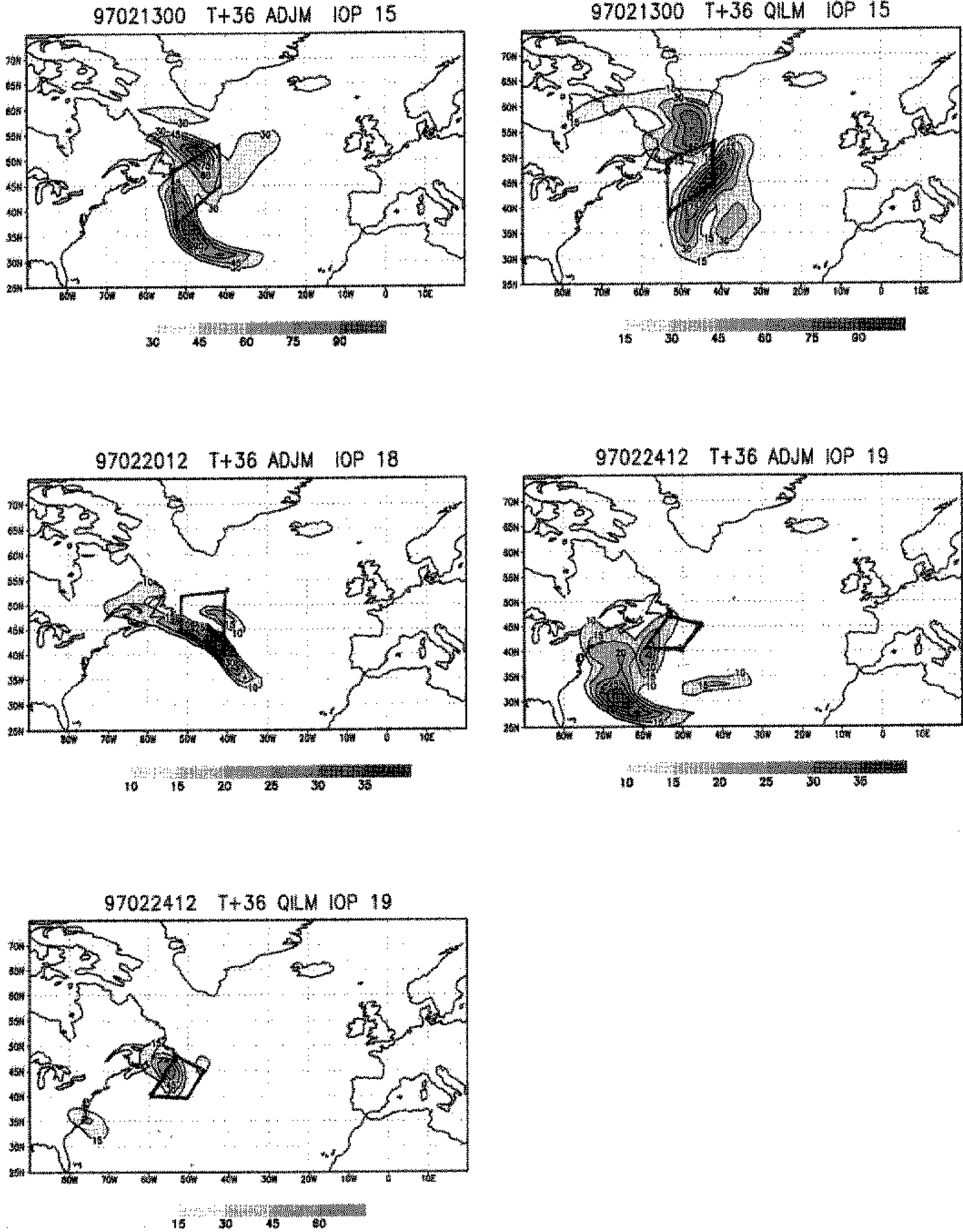


Figure 1. Continued.

flight missions. In many cases, they supported the primary NCEP guidance: the ET technique. In some cases in which the ET was not used, the QILM and/or ADJM agreed with the targeting guidance provided by the adjoint singular-vector methodologies used in one or more of the other centres (ECMWF and Meteo-France). The signal introduced by extra data at targeting time moved to the verification area at verification time.

TABLE 2. FASTEX CASES INVESTIGATED IN THIS STUDY

Intensive Observation Period	Targeting Product issued	Analysis time	Verification time	Centre of verification area	Centre of most sensitive area	Method	Forecast impact
3	1200 UTC 11 January	T+48	T+72	50°N,10°W	35–48°N,60–50°W	ADJM	Mixed
5	1200 UTC 18 January	T+48	T+72	50°N,10°W	30–40°N,60–50°W	QILM	Mixed
11c	0000 UTC 04 February	T+36	T+72	50°N,10°W	35–50°N,50–40°W	ADJM	Positive
11d	0000 UTC 04 February	T+48	T+72	50°N,10°W	35–50°N,45–30°W	ADJM	Mostly positive
13	1200 UTC 08 February	T+48	T+72	57.5°N,20°W	40–57°N,55–45°W	QILM	Mixed
14	0000 UTC 11 February	T+36	T+72	50°N,10°W	52–60°N,55–42°W	ADJM	Mixed
15	0000 UTC 13 February	T+36	T+72	50°N,10°W	40–50°N,50–40°W	ADJM QILM	Negative
16	1200 UTC 14 February	T+48	T+72	50°N,10°W	40°N,60°W	ADJM QILM	Mixed
18	1200 UTC 20 February	T+36	T+72	52.5°N,17.5°W	50°N,50°W	ADJM	Mostly Positive
19	1200 UTC 24 February	T+36	T+72	50°N,10°W	37–50°N,60–50°W	ADJM QILM	Mostly Positive

Observation and verification times are in terms of forecast lead time from time of sensitivity calculations. Sensitivity is based on real-time adjoint method (ADJM) and quasi-inverse linear method (QILM) guidances. The targeting-product-issued time may differ from Szunyogh *et al.* (1999) in some cases, since a different forecast lead time was used for the different targeting methods in the sensitivity calculations. However, the verification time is the same for all targeting techniques.

The forecast evaluation shows that only about half of the cases show positive impacts. The impact of the targeted data is also rather small. There are several possible reasons for this somewhat disappointing result: (a) The MRF control forecasts were in general good, leaving little 'room for improvement'. (b) In some cases, the flight take-off time was not the same as the chosen targeting time, and the data was used in the following 6-hour cycles. Since the SSI system is performed every 6 hours, and the data cut-off is 3 hours around the analysis time, some dropwindsonde data fell outside the cut-off time so that only part of the targeted data was used in the analysis. (c) The estimation of forecast impacts is a problem with a notoriously poor signal-to-noise ratio, given the chaotic nature of the atmosphere, and any change may result in a mixture of positive and negative impacts. (d) The FASTEX verification is in the eastern side of the Atlantic Ocean, with poor upstream data coverage. The verification region and time are selected over areas of large forecast uncertainty, making even the atmospheric analyses in these regions suspect.

Finally, the FASTEX IOPs were not always cases of strong error growth in the verification region. Pu *et al.* (1998) tested the QILM and ADJM by using actual observed forecast differences over North America from forecasts with and without dropwindsonde data over the Gulf of Alaska. Their results suggest that the QILM and the ADJM targeting are similar only for cases with large forecast impact within the verification region. For small forecast impact, the ADJM indicates areas where small changes can make a larger impact on the verification region, whereas the QILM indicates where the forecast impact actually came from. Therefore, if the targeting is performed only for cases where the ensemble shows large spread over the verification area, it can be expected that the adjoint and the inverse approaches will point to similar regions. In addition, the QILM can be used when, for example, two operational forecasts are

significantly different in the region of interest. In that case the QILM can be used to trace back to the area where those differences originate, and an analysis of the observations could be used to indicate which of the forecasts is more reliable.

ACKNOWLEDGEMENT

We would like to express our gratitude to Dr Zoltan Toth for valuable discussions and suggestions during both the real-time FASTEX and the post-analysis process, and to Prof. Kerry Emanuel and Dr Istvan Szunyogh for useful discussions during FASTEX. The assistance from Mr Timothy Marchok and Jack Woollen is also appreciated. This research was supported by the University Corporation for Atmospheric Research/NCEP Visiting Scientist Program.

REFERENCES

- Bergot, T., Hello, G., Joly, A. and Malardel, S. 1999 Adaptive observations: A feasibility study. *Mon. Weather Rev.*, **127**, 743–765
- Joly, A., Jorgensen, D., Shapiro, M. A., Thorpe, A., Bessemoulin, P., Browning, K. A., Cammas, J.-P., Chalon, J.-P., Clough, S. A., Emanuel, K. A., Eymard, L., Gall, R., Hildebrand, P. H., Langland, R. H., Lemaitre, Y., Lynch, P., Moore, J. A., Persson, P., Snyder, C. and Wakimoto, R. M. 1997 The Fronts and Atlantic Storm-Track EXperiment (FASTEX): Scientific objective and experimental design. *Bull. Am. Meteorol. Soc.*, **78**, 1917–1940
- Langland, R. and Rohaly, G. 1996 'Analysis error and adjoint sensitivity in prediction of a North Atlantic frontal cyclone'. Pp.150–152 in preprints of 11th conference on numerical weather prediction, 19–23 August 1996, Norfolk, Virginia, USA. Am. Meteorol. Soc., USA
- Lord, S. J. 1996 'The impact on synoptic-scale forecasts over the United States of dropwindsonde observations taken in the Northeast Pacific'. Pp.70–71 in preprints of 11th conference on numerical weather prediction, 19–23 August, 1996, Norfolk, Virginia, USA. Am. Meteorol. Soc., USA
- Palmer, T. N., Gelaro, R., Barkmeijer, J. and Buizza, R. 1998 Singular vector, metrics and adaptive observations. *J. Atmos. Sci.*, **55**, 633–653
- Parrish, D. F. and Derber, J. C. 1992 The National Meteorological Center Spectral Statistical Interpolation Analysis System. *Mon. Weather Rev.*, **120**, 1747–1763
- Pu, Z.-X., Kalnay, E., Sela, J. and Szunyogh, I. 1997 Sensitivity of forecast error to initial conditions with a quasi-inverse linear method. *Mon. Weather Rev.*, **125**, 2479–2503
- Pu, Z.-X., Lord, S. J. and Kalnay, E. 1998 Forecast sensitivity with dropwindsonde data and targeted observations. *Tellus*, **50A**, 391–410
- Rabier, F., Klinker, E., Courtier, P. and Hollingsworth, A. 1996 Sensitivity of forecast errors to initial conditions. *Q. J. R. Meteorol. Soc.*, **122**, 121–150
- Reynolds, C. and Palmer, T. N. 1998 Decaying singular vectors and their impact on analysis and forecast correction. *J. Atmos. Sci.*, **55**, 3005–3023
- Szunyogh, I., Toth, Z., Emanuel, K. A., Bishop, C. H., Snyder, C., Morss, R. E., Woollen, J. and Marchok, T. 1999 Ensemble-based targeting experiments during FASTEX: The effect of dropsonde data from the Lear jet. *Q. J. R. Meteorol. Soc.*, **125**, 3189–3217
- Toth, Z. 1997 Proceedings of the FASTEX upstream observations workshop, NCEP, April 10–11, Camp Springs, MD. NCEP Office Note, No. 420
- Toth, Z. and Kalnay, E. 1997 Ensemble forecasting at NCEP and the breeding method. *Mon. Weather Rev.*, **125**, 3297–3319